Vol. 2 No. 5 (2024)

Spectrum of Engineering Sciences

Online ISSN
3007-3138

Print ISSN
3007-312X

# U-Net CNN Architecture and OCR for High-Accuracy Pattern and Text Recognition in Meteorological Facsimile Data

**Syed Owais Shah**
Department of Telecommunication, Hazara University Mansehra, Pakistan Email: owais@hu.edu.pk
**Muneeba Darwaish**
Department of Telecommunication, Hazara University Mansehra, Pakistan. Email: owais@hu.edu.pk
**Muhammad Shujaat**
Department of Telecommunication, Hazara University Mansehra, Pakistan. Email: muneebadarwaish@gamil.com
**Muhammad Asad Khan***
Department of Telecommunication, Hazara University Mansehra, Pakistan. Corresponding Author Email: asadkhan@hu.edu.pk
**Mohsin Shah**
Department of Telecommunication, Hazara University Mansehra, Pakistan. Email: syedmohsinshah@hu.edu.pk

## Abstract

The categorization of meteorological data through imagery plays a vital role in weather prediction, environmental surveillance, military activities, target identification, high-altitude aviation, image retrieval, and maritime navigation. The study explores the application of machine learning through convolutional neural networks (CNNs) to derive crucial and relevant insights from weather facsimile charts. The data on weather facsimile charts is frequently identified and depicted on weather charts, relying on the expertise of forecasters. Identifying unique weather patterns from linear weather systems presents a

Vol. 2 No. 5 (2024)

Spectrum of Engineering Sciences

SPECTRUM OF ENGINEERING SCIENCES

Online ISSN
3007-3138
Print ISSN
3007-312X

significant challenge in the field of meteorological science research. This paper presents a significant contribution to pattern recognition and meteorological computing through the introduction of the U-Net Convolutional Neural Network (CNN) classification model, showcasing the effectiveness of this methodology in analyzing meteorological information. Utilizing a framework for hyper-parameter optimization based on convolutional layers, our CNN system identifies weather patterns with an accuracy ranging from 89% to 99% (Dashed Line pattern, Weather symbols). Recently, based on character recognition, Optical Character Recognition is commonly utilized in many straightforward applications. This paper presents Easy OCR, a deep learning library based on Python that includes detection models for over 85 languages. An accessible OCR method is proposed for character recognition from the weather facsimile maps dataset. The experiment demonstrates that the proposed method achieves an impressive accuracy rate of 95%-98% in the thorough and precise extraction of both textual and numerical data from weather facsimile charts.

**Keywords:** Meteorological facsimile charts; CNN; Data augmentation; Easy OCR, Pattern Recognition

## 1. Introduction

Meteorological Facsimile Chart provides precise weather information presented in the form of images. The foundation of the facsimile map information system has notably enhanced public information services and the upkeep of public services in recent years. The existing conditions and trends of fluctuations in both surface and

Vol. 2 No. 5 (2024)
Spectrum of Engineering Sciences
Online ISSN
3007-3138
Print ISSN
3007-312X

atmospheric weather over the ocean can be illustrated through the use of the meteorological facsimile map. The meteorological facsimile map (MFM) serves as a graphical representation of numerical value forecasts, enabling navigation experts to access pertinent meteorological information directly through these MFMs. This representation of weather conditions is not only intuitive but also plays a crucial role in observing, tracking, and studying the evolution and movement of weather systems. Meteorological facsimile maps provide significant assistance for navigating the ocean. Acquiring weather facsimile charts via the weather facsimile receiver stands out as one of the most efficient ways to gather weather information relevant to the ship's navigation operations. The processing of meteorological facsimile maps through image processing stands out as a crucial aspect of the latest modern weather facsimile receiver, representing a trend in forecasting future weather over the sea.

Employing image processing technology to derive essential information, like the meteorological facsimile weather map system, is conducive to integration with additional data and holds considerable practical significance in maritime weather forecasting, navigation, and military operations. The research content in digital image processing technology is extensive, focusing on the manipulation of images for various objectives. The examination of effective methods for extracting meteorological information has been ongoing for numerous years, and undoubtedly, progress has been achieved. Numerous studies have explored the implementation of interactive displays such as fax maps, radar charts, and digital charts for maritime

Vol. 2 No. 5 (2024)

Spectrum of Engineering Sciences

Online ISSN
3007-3138

Print ISSN
3007-312X

defense [1], as well as forgery detection for navigation in oceanic contexts [2]. Various algorithms have been proposed to extract and identify different valuable information (isobars, isotherms, frontal lines, numerical data) from meteorological facsimile maps [3-5]. An alternative method explores the algorithm of meteorological facsimile map vectorization to extract dynamic information present in the map, including numbers, letters, and various symbols. This addresses numerous constraints associated with conventional meteorological facsimile charts, such as challenges in processing and preservation.

Recent advancements in deep learning have yielded significant and promising outcomes in pattern recognition challenges, exemplified by the ImageNet Large Scale Visual Recognition Challenge [6]. Furthermore, deep learning techniques have emerged as a powerful method for analyzing weather events on maps, such as weather fronts [7]. This study highlights several challenges associated with automatic information recognition from meteorological maps. The weather information presented in meteorological facsimile charts is significantly more intricate and complex compared to the data found in topographic maps, making it challenging to extract and identify. Second. Another challenge for this study is the lack of sufficient data that is not publicly available, which is required for the CNN model. CNN excels in addressing intricate topics like natural language processing, image classification, and speech recognition. Our investigation centers on the influence of image data through deep learning techniques to extract and identify crucial and

Vol. 2 No. 5 (2024)
Spectrum of Engineering Sciences
Online ISSN
3007-3138
Print ISSN
3007-312X

dependable features from meteorological facsimile maps, including weather system symbols, dashed lines, and characters.

This paper features a formulation of the problem concerning the detection of meteorological information using deep learning techniques. We implement a system for deep learning image transformations based on the architecture presented in [8], which represents one of the neural network frameworks utilized for image segmentation. Our advanced neural networks have mastered the transformation process, enabling the automatic detection and identification of specific information from intricate sets of maps, whether dealing with single or multiple data quantities. We investigate the suggested methodology and present initial findings of critical data in the detection and recognition of weather facsimile maps for each physical quantity.

## 2. Review of Related Work

The study of automatic identification and extraction of information from maps has a rich history and encompasses a diverse range of methods applicable to different types of maps. An interesting observation regarding the shapes of meteorological weather systems in official weather charts is that numerous significant weather events are represented as lines. Fronts, troughs, and ridges inherently possess a line-shaped characteristic, and even pressure extrema, whether high or low, along with tropical cyclones, can be conceptualized as entities defined by lines. The identification of patterns in meteorological fields frequently involves ridge lines or narrow zones characterized by relatively high or low values. This

Vol. 2 No. 5 (2024)

Spectrum of Engineering Sciences

SPECTRUM OF ENGINEERING SCIENCES

Online ISSN
3007-3138

Print ISSN
3007-312X

document presents an approach for the automatic detection of such features, utilizing input fields provided on regular grids [9]. The proposed algorithm extracts and recognizes frontal lines and provides numerical identification of contours from meteorological facsimile maps [10]. The extraction and separation of the cordon are conducted in accordance with the characteristics of the meteorological facsimile diagram, utilizing morphology expansion and the skeleton extraction method [11]. To integrate the meteorological facsimile diagram with additional navigational information, data is extracted from the meteorological facsimile map and the information storage structure is designed [12]. A method was proposed for extracting frontal line symbols from weather facsimile images using external rectangles [13]. There is a scarcity of literature focused on automating the identification of line-shaped weather systems, including contours, fronts, troughs, and ridges. A considerable number of studies have been conducted on the analysis of digitized maps and drawings, yet a significant portion focuses on the extraction of lines, characters, or symbols. A variety of methods succinctly outline the procedure for map digitization along with a straightforward algorithm [14]. A cartography and graphics-based approach was suggested to derive contours by removing other symbols and layers based on the analysis of various characteristics [15]. A cartographic pattern recognition system utilizing homogeneous parallel algorithms [16] and an automated map recognition system represent some of the initial efforts in the field of map recognition [17]. Furthermore, numerous methodologies

Vol. 2 No. 5 (2024)
Spectrum of Engineering Sciences
Online ISSN
3007-3138
Print ISSN
3007-312X

emphasize symbol recognition [18], as well as the interpretation of characters from topographic maps [19].

Although considerable work has been accomplished for [20], hydrographically corrected contours have been extracted for the US Geological Survey from the US Topo product [21]. Identifying features on maps relies heavily on color information, which is crucial for effective image segmentation [22],[8]. Proposed a segmentation algorithm based on fuzzy clustering to extract characters and lines from color map images [23] (conclusion used for claim), but it does not address color aliasing and false colors inherent in topographic maps. Consequently, its performance on topographic maps, characterized by thin and closely spaced feature geometries, may be suboptimal. To enhance the results of color image segmentation, a relaxation algorithm along with morphological and filtering operations was introduced to extract contours from topographic and military topographic maps [24]. Technique for map segmentation, enhancing and identifying thin-line features utilizing multi-scale information [25].

Most map analysis techniques are conducted on binary maps characterized by thicker features that are spaced far apart from one another [26] (conclusion used for claim). Only a limited number focused on colour images and thin, closely spaced linear features [27]. Recognition in Geographic Information Systems (GIS) is demonstrated using symbolic knowledge derived from the map's legend to facilitate geographic symbol identification [28]; however, it falls short of delivering comprehensive map recognition. Yamada introduced the

Vol. 2 No. 5 (2024)

Spectrum of Engineering Sciences

Online ISSN
3007-3138

Print ISSN
3007-312X

MAP (Multi-Angled Parallel) operation, which extracts line drawings of various shapes through the iterative application of erosion-dilation operations and parallel MAP matching for symbol recognition [29],[30] (lines and symbols). Recent studies have shown various methods for distinguishing features like text and graphics in maps [31],[32],[33]. The implementation of OCR-based recognition utilizing Artificial Neural Networks (ANN) establishes a framework for the isolation and identification of contiguous and overlapping alphanumeric characters [34]. Employing connected component analysis and the Hough transform with a novel algorithm for the automated separation of text strings, which demonstrates a degree of independence from variations in font style, size, and string orientation [35].

Some of them focus on the recognition of dashed lines in engineering drawings and maps [36]. Lines serve as the fundamental graphical elements in line drawings broadly, and are especially significant in maps and scientific illustrations [37]. More advanced techniques, such as the Hough transform, perceptual grouping, and morphological operations, are among the most frequently utilized algorithms for the extraction and detection of lines and geometric shape symbols in image processing. Nonetheless, the effectiveness of these systems remains either unclear or only partially documented by the developers. Nonetheless, there has been a scarcity of studies focused on the automatic identification of line-shaped weather information within meteorological facsimile maps. The situation becomes increasingly complex when it comes to identifying and detecting objects in multiple quantities. We have applied advanced

Vol. 2 No. 5 (2024)

Spectrum of Engineering Sciences

Online ISSN
3007-3138

Print ISSN
3007-312X

learning models to address the limitations in computer vision, aiming to elucidate the complexity, overlap, and intersection of information in fax maps. This study demonstrates that neural networks represent a generative method applicable to various meteorological data.

## 3. Facsimile Data

In this research, we addressed a significant challenge related to extracting information from facsimile maps. This paper presents the inaugural creation of a dataset comprising meteorological facsimile maps. A total of 4000 images were gathered from various meteorological agencies and the NOAA central Library. Some of the collected images are illustrated in Figure 1. For the purpose of machine learning, we transformed the data into uniform grids of 512 × 512. The training data consists of original images of maps where multiple relevant variables, including dashed lines and symbols, are layered over a specified area that encompasses various pieces of information. To create the ground truth for dashed line patterns and symbolic information, we employ connected component analysis along with manual efforts. The phrase “ground truth” denotes the accurate response for supervised learning in this context. Nonetheless, it is feasible to replace it with alternative front data based on the intended objective. The source of the data, along with its spatial and temporal resolution, is presented in Table 1.

Vol. 2 No. 5 (2024)

Spectrum of Engineering Sciences

SPECTRUM OF ENGINEERING SCIENCES

Online ISSN
3007-3138
Print ISSN
3007-312X

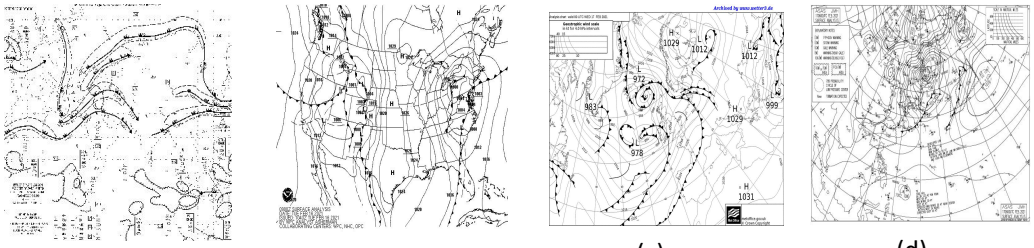

(a) (b) (c) (d)

***Figure 1: Simple Dataset Images***

**Table 1:** ***Facsimile Data Sources***

| Facsimile Maps Dataset | Time Frame | Temporal Resolution | Spatial Resolution |
|---|---|---|---|
| NOAA [40] | 1979-2021 | 24 hourly | 784x562 |
| Japan Meteorological Agency [43] | 1996-2021 | 24 hourly | 600x512 |
| Aviation Weather Chart Achieve [41] | 1991-2021 | 12 hourly | 1772x1072 |
| United Kingdom Meteorological [42] | 1990-2021 | 4.0hpa Interval Daily | 1071x759 |

## 4. Methodology

### *4.1 Convolutional Neural Network*

A Deep Neural Network typically comprises a series of convolutional layers complemented by several fully connected layers. Subsampling, such as max pooling or mean pooling, is generally performed between two consecutive convolutional layers. The researchers highlighted the significance of max pooling, contending that it could potentially be substituted by a convolutional layer in gradual increments, thereby enhancing the network architecture. In either case, the input of the Convolutional Neural Network is $(m, n, p)$ images,

Vol. 2 No. 5 (2024)

Spectrum of Engineering Sciences

Online ISSN
3007-3138

Print ISSN
3007-312X

where m and n are the image's pixel height and width, and p is the pixel's colour channel number. The CNN product is a vector of $q$ probability units (category scores) that represent the number of classes to be classified (e.g. binary classifier $q = 2$).

The CNN layers compute a convolution process between the input image and kernels (or feature maps from the previous layer). Normally, a CNN layers contain $k$ kernels (filters) with the size $(i, j, p)$, where $i, j$ are the height and width of the kernels. The sizes of the kernels are generally smaller than the width $m$ and height $n$ of the input image $p$ is often the same as the number of colour channels of the input image (e.g. a colour image has three channels: red, green, and blue). Each filter is individually wrapped with input images (or previous layer feature maps) preceded by a non-linear transformation, which describes the feature maps that are a reference for the next layer. In the convolution phase, a dot product operation is computed between the filter and the local region that's connected to the input image (or feature map from the previous layer). These learnable filters are the parameters of the convolutional layers.

The convolutional layer is the extractor of features, because the kernels drag across all inputs and generate greater outputs for certain sub-regions than for others. This allows the details to be retrieved from the inputs and stored in the feature maps that are transferred to the next layer, irrespective of where the feature is located in the input layer. The feature maps are subsampled by a pooling layer generated from a convolutional layer over an $(s,t)$ adjacent region, where $s$ $t$ is the width and height of the subsampling window. This results in the

Vol. 2 No. 5 (2024)
Spectrum of Engineering Sciences
Online ISSN
3007-3138
Print ISSN
3007-312X

feature maps achieving greater depth as the CNN increases in layers. All feature maps serve as profound representations of input data within convolutional neural networks. Every hidden unit from the preceding layer is linked to the fully connected layer. The final layer in the Convolutional Neural Network architecture, the fully connected layer, facilitates high-level reasoning by utilizing the feature vectors from the preceding layer and delivers the ultimate class scores for the image objects. The majority of current deep neural networks employ backpropagation as their learning algorithm. The back propagation algorithm aims to minimize the loss function of the weight space function through a gradient descent approach. The final total loss is distributed among each neuron in the network, leading to adjustments in the weights of neurons that exhibit significant loss. This process involves backpropagating the error from the output to the input throughout the entire network.

### *4.2 Hyper-parameter Optimization*

Training deep neural networks is often viewed as a challenging task, given the complexity and high costs associated with both the training and validation processes. Training deep neural networks efficiently and accurately necessitates a substantial amount of training data, along with meticulous optimization of model hyper-parameters, such as learning rates and regularization factors. Nonetheless, the process of tuning parameters can often be complex and time-consuming. Optimizing hyper-parameters involves identifying a specific set of parameters for a network that produces the most favourable validation outcomes. Training a deep neural network is not only a

Vol. 2 No. 5 (2024)
Spectrum of Engineering Sciences
Online ISSN
3007-3138
Print ISSN
3007-312X

costly process in terms of time, but also a rather vague operation regarding how the network's performance relates to its hyper-parameter inputs. A significant benefit of deep learning architectures is their ability to learn complex nonlinear functions. Rectified Linear Unit (ReLU) activation functions [44] are frequently utilized within the convolutional layers of deep CNNs. ReLU is favoured due to its faster learning and training characteristics compared to other activation functions like tanh.

### *4.3 CNN Configuration*

This study presents the U-Net architecture, a fully convolutional neural network that was initially proposed for addressing challenges in biomedical image segmentation [45]. This convolutional network is capable of producing optimal image segmentations even with a limited number of training images. The U-net is a neural network architecture characterized by two parallel pathways: one serving as the encoder and the other as the decoder. Every block within the encoder and decoder comprises distinct sub-layers (Fig. 2). The contracting pathway consists of iterative applications of convolutions, max pooling, activation functions, and dropout operations to derive crucial features from the input image. The expanding path produces high-resolution image features through the integration of low-resolution image features and derives predictions from the contracting path. This process encompasses several layers of repetitive transposed convolution, convolution operations, dropout, and concatenation.

Vol. 2 No. 5 (2024)

Spectrum of Engineering Sciences

SPECTRUM OF ENGINEERING SCIENCES

Online ISSN
3007-3138
Print ISSN
3007-312X

### *4.4 The Contracting Path*

The suggested network architecture generally features a contracting path. In this architecture, the contracting path consists of six blocks, each of which has four layers. Each block consists of an initial pair of convolutional layers featuring kernels (filters) of. The stride, which indicates the number of convolution steps to skip, is set to two. A rectified linear unit (ReLU) serves as the activation function in every convolutional layer, subsequently followed by Batch Normalization. These layers extract the features of the input image. Each boundary of the image pixels is zero-padded by one pixel for all convolutional layers in this architecture, ensuring that the output feature map is the same size as the input. The weights and biases associated with convolutional layers represent crucial sets of parameters that can be learned during the training process. The values of the kernels serve as weights. A further parameter bias is introduced following the output of the feature maps before it is passed to a ReLU, which serves as a nonlinear activation function. Figure 2 illustrates the arrangement of every convolutional layer. Within each block, the third layer consists of a 2 x 2 max pooling layer, which effectively diminishes the number of parameters by reducing the size of the matrix. For instance, the initial dimensions of the image are, and it was decreased to the following the first max pooling layer. The fourth layer of the last two blocks consists of a dropout layer. This approach effectively mitigates the overfitting issue by randomly omitting nodes during the training phase. The dropout estimate is 0.5, indicating that 50% of the nodes will randomly drop out.

Vol. 2 No. 5 (2024)
Spectrum of Engineering Sciences
Online ISSN
3007-3138
Print ISSN
3007-312X

Following the extraction of the initial contracting block, the specifications are forwarded to the subsequent contracting block, and the process is executed for each block. At the same time, following each block, the quantity of kernels doubles, allowing the architecture to effectively learn intricate image features. After the fourth contracted block, two padded convolutional layers with kernels are present. Every component is paired with a ReLU activation function, which facilitates the interaction between the contracting and expanding pathways.

### *4.5 The Expanding Path*

In the expanding direction, there are four blocks, each consisting of five layers (Figure. 2). The initial layer consists of a transposed convolution layer, also known as a deconvergence layer, for each block in the expanding block. This layer is designed to up-sample the feature maps from low resolution to high resolution. The kernel size is defined, and the stride is set to 2, with one pixel of zero-padding in the transposed convolutional layers. The initial transposed convolutional layer features an input dimension of 8 x 8, resulting in an output dimension of 16 x 16. In every expanding block, each second layer serves as a concatenation layer that merges the feature maps at the same level from the contracting path with those from the expanding path. This action retrieves localization information from the contracting path and aids in reconstructing high-resolution feature maps in the expanding path. Every expanding block's third layer functions as a dropout layer, operating in parallel with the corresponding layer in the contracting path. Each expanding block

Vol. 2 No. 5 (2024)
Spectrum of Engineering Sciences
Online ISSN
3007-3138
Print ISSN
3007-312X

incorporates padded convolution layers in the fourth and fifth layers, featuring kernels with a stride of 1.

In every convolutional layer, the activation function utilized is a ReLU. Compared to the contracting blocks, the number of kernels following each expanding block has been reduced by half. The parameters are transmitted to the subsequent block following the expansion of the first block, and the process is reiterated. The size of the figure after four expansion blocks remains consistent with the original size. Continuing along the defined trajectory, the output layer consists of a padded convolutional layer featuring a kernel and a stride of 1.

The Sigmoid activation function [46] is employed to represent the output as a probability ranging from 0 to 1. The neural network subsequently computes the loss function by assessing the average discrepancy between the anticipated values and the actual subsurface interface models. A lower value of the loss function indicates a higher accuracy in predictions. The parameters of the model, including kernel weights and biases, are subsequently determined through the application of an optimization algorithm aimed at minimizing the loss function. The model training process outlines the Deep CNN architecture and layer parameters as detailed in Table 2.

Table 2: Deep CNN architecture and layer parameters. The convolutional layer parameters are denoted as <filter size>-<number of feature maps> (e.g. 3x3-64). The pooling layer parameters are denoted as <pooling window> (e.g. 2x2). The fully connected layer parameters are denoted as <number of units> (e.g. 2).

Vol. 2 No. 5 (2024)

Spectrum of Engineering Sciences

Online ISSN
3007-3138

Print ISSN
3007-312X

**Table 2:** ***Architecture details of the proposed CNN model***

| | Conv1 | Pooling | Conv2 | Pooling | Skip Connection | Output |
|---|---|---|---|---|---|---|
| Dashed Lines | 3x3-64 | 2x2 | 3x3-128 | 2x2 | 1x1 | 512x512 x1 |
| Symbols | 3x3-64 | 2x2 | 3x3-128 | 2x2 | 1x1 | 512x512 x1 |

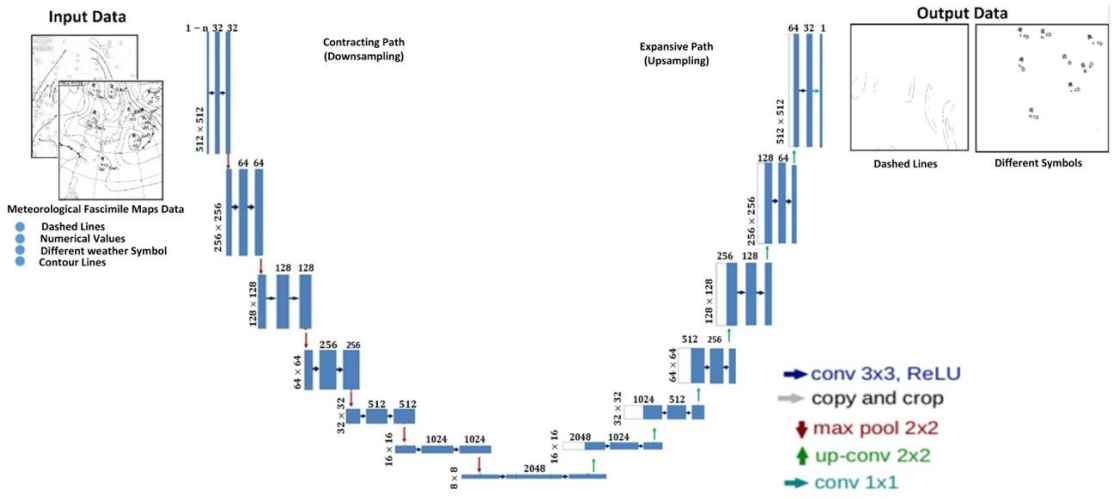


***Figure 2: Architecture of the proposed U-Net convolutional neural network.***

### *4.6 Dataset Preprocessing*

The meteorological facsimile data is generated and stored in image format. The extraction and recognition of dashed lines as meteorological information involves dividing our dataset into 2400 (60%) for training, 800 (20%) for validation, and 800 (20%) for testing. To recognize symbols, we utilize data from 400 images, allocating 80% for training and 20% for the validation set, as detailed in Table 3.

Vol. 2 No. 5 (2024)

Spectrum of Engineering Sciences

SPECTRUM OF ENGINEERING SCIENCES

Online ISSN
3007-3138
Print ISSN
3007-312X

The training set is first utilized to assess the parameters of the neural network model. The validation dataset is subsequently utilized to assess the efficacy of the neural network model derived from the training dataset, in addition to identifying any potential overfitting of the model to the training data. The final neural network model undergoes evaluation with the test dataset, which remained untouched during the training phase.

To enhance the model for symbol extraction, we implement data augmentation techniques. Among the basic transformations utilized in image processing are geometric transformations like flipping, translation, rotation, cropping, and scaling. Augmentation offers a set of methods designed to enhance both the quality and quantity of training datasets, facilitating the development of effective Deep Learning models while also mitigating the risk of model overfitting.

**Table 3:** ***Size Of Image Patch And The Number Of Annotated Datasets Used In The Proposed Model***

| Variables | Image Dimension | Total Examples | Training Set | Validation Set | Testing Set |
|---|---|---|---|---|---|
| Dashed Lines | 512x512 | 40000 +ve 4000-ve | 2400+ive 2400-ive | 800+ive 800-ive | 800+ive |
| Symbols | 512 x 512 | 500+ve 500-ve | 400+ive 400-ive | 100+ive 100-ive | 100+ive |

Vol. 2 No. 5 (2024)

Spectrum of Engineering Sciences

SPECTRUM OF ENGINEERING SCIENCES

Online ISSN
3007-3138
Print ISSN
3007-312X

### 4.7 *OCR (Optical Character Recognition)*

Easy OCR stands out as the most straightforward method for implementing Optical Character Recognition. EasyOCR has the capability to handle multiple languages simultaneously, as long as they are compatible with one another. The extraction of characters and text from meteorological map images presents significant challenges due to the intricate backgrounds and the variability in shape, size, and orientation. Although the significance of this area has motivated numerous scholars to concentrate on it and various experiments on character extraction have been carried out, they remain limited to simplified contextual conditions. Our approach involved utilizing an edge-based technique alongside mathematical morphological operations for localization, complemented by an OCR technique for recognition.

### 4.8 *Image Pre-Processing*

In this section, we will initially acquire an image from which we need to extract information, followed by the process of rescaling the image. We enlarge our image to better identify the finer details of the information, such as text and numbers. To avoid processing overload, transform the colored image into a grayscale version. Following the conversion of an image to grayscale, morphological operations are then applied to the image. Initially, dilation is performed, followed by the application of erosion to the image.

Spectrum of Engineering Sciences
SPECTRUM OF ENGINEERING SCIENCES
Online ISSN
3007-3138
Print ISSN
3007-312X

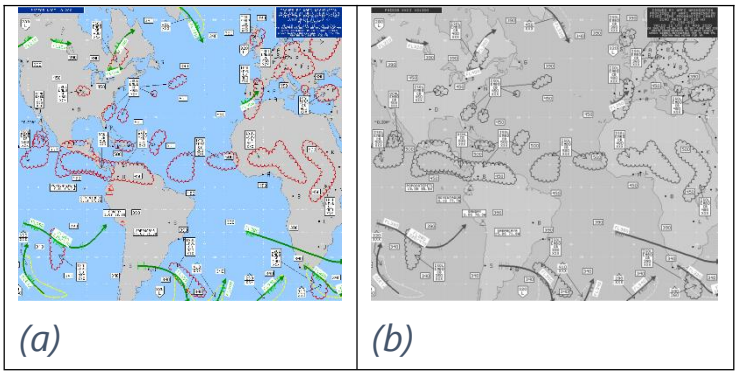

(a) (b)

***Figure 3: (a) Original image, (b) Grayscale image***

### *4.9 Extraction and Localization*

In this subsection, we initially convert a grayscale image into a binary image by determining the appropriate threshold. We then apply morphological transformations through dilation and erosion, as illustrated in Fig. 4 (a). Dilation and erosion are established techniques in the field of image processing. The quantity of pixels that are either added or removed from objects within an image is influenced by the dimensions and configuration of the structuring element employed in the image processing task. A bilateral filter is utilized as a non-linear, edge-preserving, and noise-reducing smoothing technique for images. It substitutes the intensity of each pixel with a weighted average derived from the intensities of neighbouring pixels, following a Gaussian distribution as illustrated in figure 4 (b).

Vol. 2 No. 5 (2024)

Spectrum of Engineering Sciences

SPECTRUM OF ENGINEERING SCIENCES

Online ISSN
3007-3138

Print ISSN
3007-312X

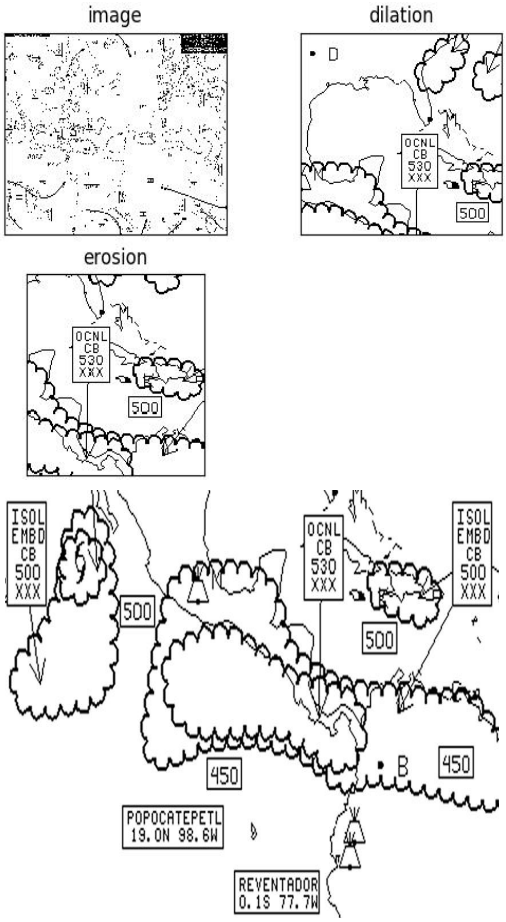


***Figure 4: (a) Morphological Transformation (b) Applying threshold and bilateral filter***

We determine the structural variable in accordance with the cluster of image text and numbers using EasyOCR library [47] for to extraction and localization of text and numbers as shown in Fig. 5.

Vol. 2 No. 5 (2024)
Spectrum of Engineering Sciences
SPECTRUM OF ENGINEERING SCIENCES
Online ISSN
3007-3138
Print ISSN
3007-312X

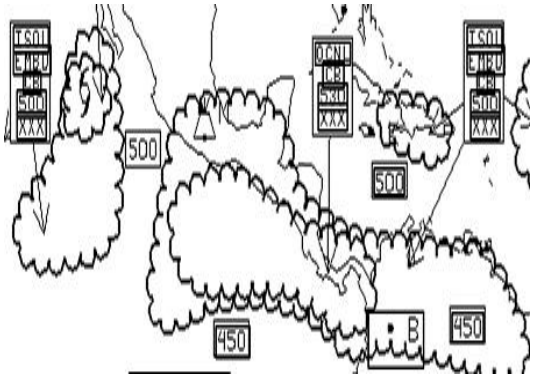


***Figure 5: Localization of text/Alphanumeric***

### *4.10 Easy OCR (Optical Character Recognition)*

In recent decades, numerous libraries globally have initiated efforts to digitize their complete map collections to facilitate easier access to the information contained within these maps. OCR seeks to identify optical patterns, typically present in digital images, that correspond to alphanumeric characters and other symbols. Optical character recognition (OCR) techniques are frequently employed for the digitization of text from printed documents. Recent literature primarily concentrates on extracting textual information from documents, with a notable scarcity of focus on meteorological maps. Meteorological facsimile maps are rich in text and alphanumeric features that convey numerical information relevant to the field of meteorology. This study aims to establish the application of an OCR method for recognizing numerical and textual data from facsimile charts, which could ultimately facilitate the automated generation of information within the meteorological field. The Easy OCR package allows for effective character recognition from maps. The methodology framework is illustrated in the figure below (Figure 6).

Spectrum of Engineering Sciences
Online ISSN
3007-3138
Print ISSN
3007-312X
SPECTRUM OF ENGINEERING SCIENCES

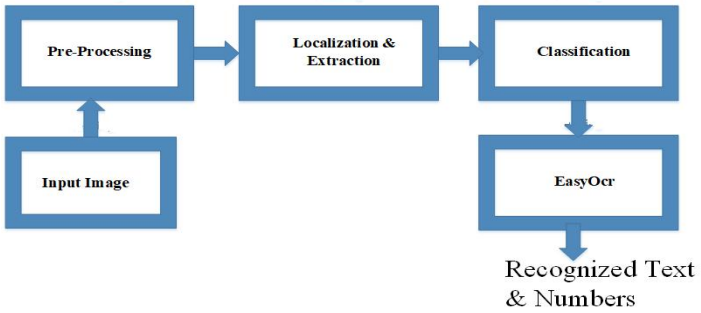


***Figure 6: Flowchart of the Text/Numeric Recognition Methodology using EasyOCR***

## 5. Experimental Results and Discussion

In the following, an overview of the research areas is presented, including the utilized data sets and their normalization. The results of the achieved recognition rate for meteorological facsimile maps are then discussed. The evaluation of the classification method was conducted on a range of temporal resolution maps. The selection of research areas was influenced by the accessibility of meteorological information maps provided by various meteorological agencies. To assess the accuracy of the classification method for dashed line patterns and symbolic information, our proposed deep CNN architecture has attained a relatively high accuracy of 85-95%, as summarized in the Table 6.

Moreover, the system's design is resilient against overfitting. Based on the proposed CNN, we believe this is primarily attributed to the ample quantity and adequate scale of our dataset. The training and test classification performance indicates that the proposed CNNs effectively learn pattern representations from classified data and can make inferences based on the features acquired. The conventional threshold-based detection approach generally requires a human

Spectrum of Engineering Sciences
Online ISSN
3007-3138
Print ISSN
3007-312X

expert to meticulously analyze the different variations of diverse information. In comparison, this study demonstrates that the proposed CNNs can effectively learn various patterns on maps utilizing labeled data, thus eliminating the need for subjective thresholds. Character recognition has emerged as a prominent area of investigation for retrieving textual information in contemporary studies.

This paper provides an overview of the different existing approaches for character recognition from various maps and drawings. In addition to the comparison, they have attained a commendable recognition rate; however, they exhibit a low recognition rate for touching text/characters and produce maps of poor quality [31],[32],[34]. A promising character recognition system has been implemented for meteorological facsimile maps, which includes the pre-processing of maps. The Easy OCR algorithm we developed allowed for effective character recognition from maps. The results indicate that utilizing a combination of various types of functions yields the highest recognition rate. The highest recognition rate for numeric and alphanumeric characters achieved is 96.66%, while the recognition rate for text/characters is approximately 90%. Misclassification in certain maps arises from the identification of undesired characters.

Spectrum of Engineering Sciences
Online ISSN
3007-3138
Print ISSN
3007-312X

**Table 4:** ***Overall Classification Accuracy***

| Variables | Train | Test | Methodology | Train time |
|---|---|---|---|---|
| Dashed Lines Pattern | 99.90% | 95%-97% | CNN(U-Net) | ≈ 2 Hours |
| Different Symbols | 99.85% | 85-99% | CNN(U-Net)+Augmentation | 1 Hours |
| Character Recognition | 99% | 90-96% | Easy OCR | 1 Hours |

### *5.1 Classification Results for Dashed Lines*

This study proposed a deep CNN for the first time to extract and recognize the dashed line pattern from the complex line-shaped information of meteorological facsimile maps, compared to various existing traditional techniques for recognition of different information features from these maps [4],[3],[5],[48],[2],[38]. The proposed approach focuses on pixel-based classification, assigning each pixel to a specific class within meteorological maps. It effectively tackles issues related to contour lines that are narrow, closely spaced, and exhibit intersections and overlaps among features. Figure 7 illustrates instances of weather maps generated by simulation models that have been accurately categorized by deep convolutional neural networks.

Vol. 2 No. 5 (2024)

Spectrum of Engineering Sciences

SPECTRUM OF ENGINEERING SCIENCES

Online ISSN
3007-3138

Print ISSN
3007-312X

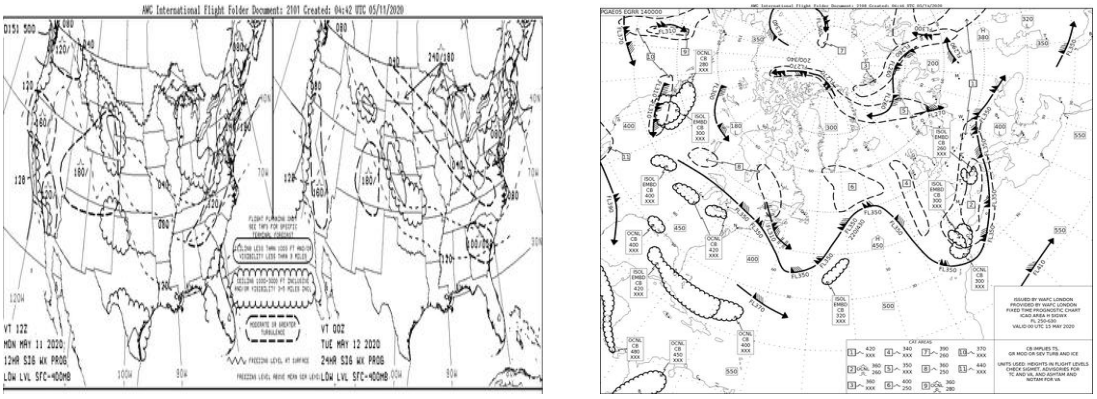

***Figure 7: Meteorological Facsimile Map for CNN Classification***

Among the various types of meteorological information patterns, line-shaped weather systems exhibit the most comprehensive geographical patterns compared to other existing proposed theories for dashed line detection for different objectives, as shown in Table 5. In Fig. 8, the pattern of dashed lines is clearly defined and accurately classified by our proposed model. This distinction is evident when compared to other multiple patterns that contain specific information related to the interacting dashed lines. Dashed line patterns are straightforward to grasp and are effectively represented within CNN due to their uniform and recognizable traits. The extraction and identification of dashed lines from a meteorological facsimile chart yielded impressive results, with our deep CNNs achieving nearly optimal classification accuracy of 96%.

Vol. 2 No. 5 (2024)

Spectrum of Engineering Sciences

SPECTRUM OF ENGINEERING SCIENCES

Online ISSN
3007-3138
Print ISSN
3007-312X

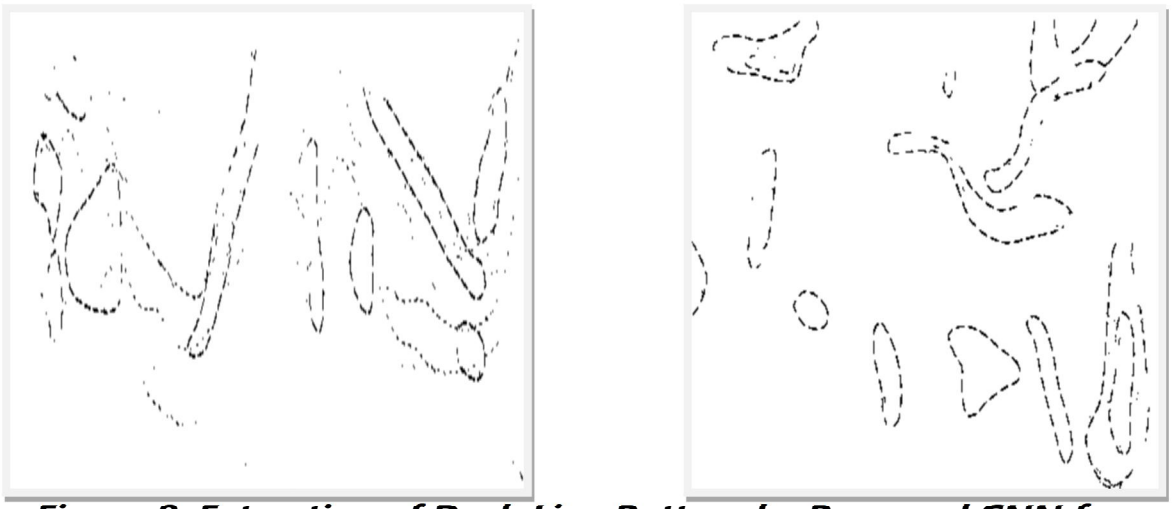

***Figure 8: Extraction of Dash Line Pattern by Proposed CNN from Complex Meteorological Map***

**Table 5:** ***Comparison of Dashed Line Recognition Methods***

| **Methods** | **Type of image/Map** | **Shortcoming** | **Performance** |
|---|---|---|---|
| Morphological Approach [39] | Binary Dashed lines image of engineering drawing | For Twisting and multi-directional lines false detection occurred | 85% |
| MAP (Multi angled parallelism) [30] | Topographic Map | limitedly reported by the system | 90% |
| Hough Transform [38] | Simple Image contain different lines | False detection occurred for horizon dashed | 85% |

Vol. 2 No. 5 (2024)

Spectrum of Engineering Sciences

Online ISSN 3007-3138

Print ISSN 3007-312X

| | | | |
|---|---|---|---|
| | | lines | |
| Map Digitization Process [14] | paper -based geographical maps | Poor performance on complex Maps | 80% |
| Combining Force Histogram [36] | Technical documents | more complex repetitive patterns of dashed lines | About to 70% |
| vector-based Recognition [37] | Technical drawing image | overlapping with Text Generate false detection | 70% |
| perceptual grouping [18] | IGMI maps | Due to Folded and Thick dashed Lines | 75-95% |
| **Proposed Method** | Meteorological facsimile maps | | 95-96% |

### *5.2 Classification Results for Symbols*

The information presented on meteorological maps is predominantly symbolic, lacking a thorough comprehension of the area they depict. Retrieving information from archival charts, whether they are hand-drawn or printed, is frequently essential. In contrast, meteorological weather maps incorporate various types of symbolic information that differ in scale and orientation against a complex background, as illustrated in Fig 9. A symbol is a crucial element of a meteorological

Vol. 2 No. 5 (2024)

Spectrum of Engineering Sciences

SPECTRUM OF ENGINEERING SCIENCES

Online ISSN
3007-3138
Print ISSN
3007-312X

facsimile chart for accurately extracting meteorological information from the chart [10],[48].

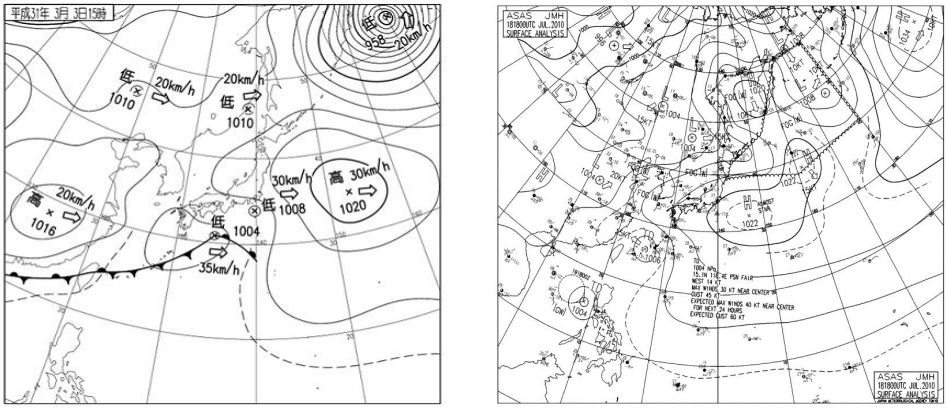

***Figure 9: Japan Meteorological Information Chat***

Table 6 presents various existing theories that have introduced algorithms aimed at recognizing symbols from topographic maps, particularly for applications in Geographic Information Systems (GIS). In addition, our proposed model is capable of identifying meteorological symbols from weather facsimile maps, which convey essential meteorological information within the field. To train our model with a dataset containing fewer images, we employ data augmentation techniques to generate sufficient data for accurate and meaningful predictions. The system utilizes data gathered from the Japan Meteorological Agency (JMA), and the distribution used for model training is presented in the table 6. Our network achieved an impressive accuracy rate of over 85-99% in symbol recognition. The misclassification and reduced recognition rate stem from the limited number of images in the dataset. Figure 10 illustrates instances of

Vol. 2 No. 5 (2024)

Spectrum of Engineering Sciences

Online ISSN
3007-3138

Print ISSN
3007-312X

symbols that have been accurately identified by the model in meteorological maps.

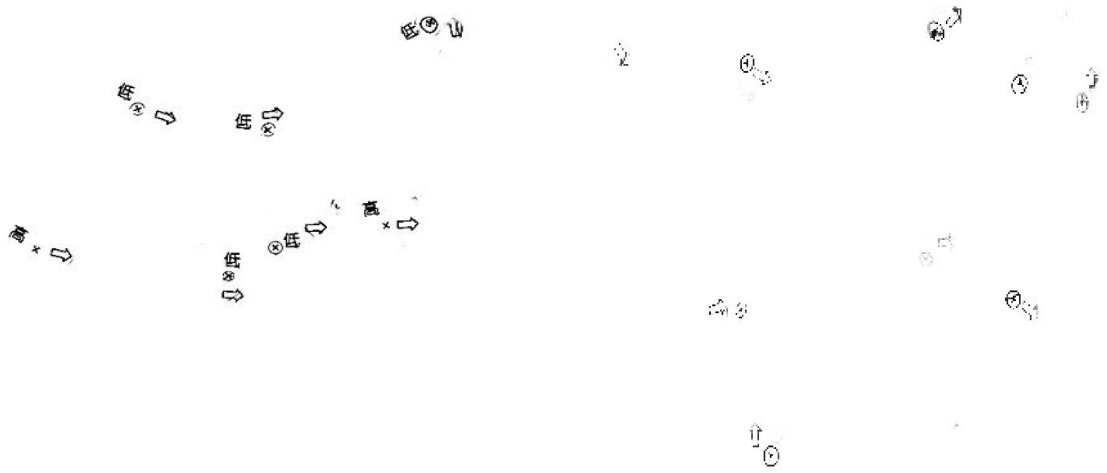

***Figure 10: Extraction of Dashed Lines pattern by proposed CNN from Meteorological Information Chart***

**Table 6:** ***Comparison of Symbol Recognition Methods on Maps***

| **Methods** | **Type of image/Map** | **Weakness** | **performance** |
|---|---|---|---|
| MAP(multiangled parallelism) [30] | Topographic Map | negative information and low resolution of symbols | 70% |
| Statistical pattern recognition [28] | GT3 map of Finland | Limited to some | 92% |

Spectrum of Engineering Sciences
SPECTRUM OF ENGINEERING SCIENCES
Online ISSN
3007-3138
Print ISSN
3007-312X

| | | | |
|---|---|---|---|
| | | portion of map | |
| Map Digitization Process [14] | paper -based geographical maps | Complexity of Map /limited to very simple geometrical shapes | 85% |
| perceptual grouping [18] | IGMI maps | Poor matching of symbols | 90% |
| Template Matching [19] | Topographic map | Complexity and wide variation. | 84.68% |
| **Proposed Method** | Any kind of weather facsimile map | Limited amount of Label Data | 85%-99% |

### *5.3 Classification Results for Text and Numbers*

Textual and numerical features offer significant insights in the meteorological map. The textual and numerical information from the meteorological map interacts and is influenced by the complex patterns of facsimile maps, which have overlapping intersections with various orientations and scales, making it challenging to extract and recognize, as illustrated in Fig 11. The reported work [10],[48] extracts and recognizes numeric features; however, the recognition rate is low and lacks emphasis on alphanumeric characters.

Vol. 2 No. 5 (2024)

Spectrum of Engineering Sciences

Online ISSN
3007-3138

Print ISSN
3007-312X

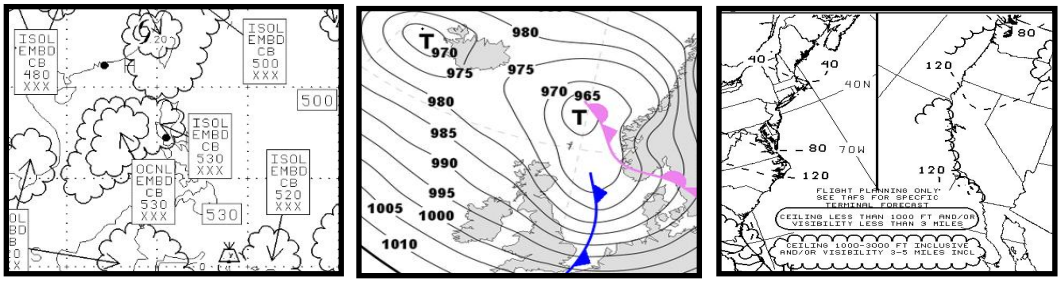


*Figure 11: Text and Numeric Information from Meteorological Map*

However, in comparison to current techniques for various types of maps [31, 32],[33],([34] the overall accuracy of the algorithm is regarded quite favorably for each map. The system under discussion underwent testing with a dataset comprising 4000 images of meteorological facsimile maps. The proposed algorithm effectively extracts and recognizes textual information as well as numeric and alphanumeric characters from the map, as illustrated in the figure 12. The developed algorithm demonstrates an impressive recognition rate of approximately 90%-96%, accompanied by a notably low error rate.

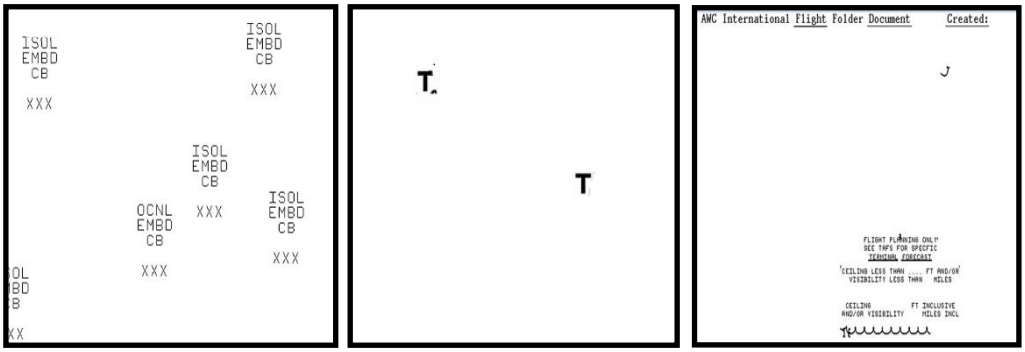


***Number/Alphanumeric Recognition***

Vol. 2 No. 5 (2024)

Spectrum of Engineering Sciences

SPECTRUM OF ENGINEERING SCIENCES

Online ISSN
3007-3138

Print ISSN
3007-312X

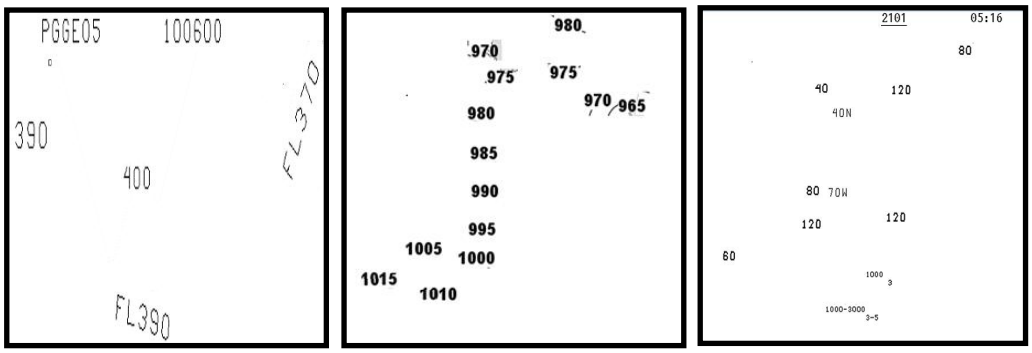


***Figure 12: Text and Numeric Pattern Recognition using Proposed Method***

**Table 7:** ***Comparison of Text and Numeric Recognition Methods on Maps***

| **Methods** | **Type of image/Map** | **Weakness** | **performance** |
|---|---|---|---|
| OCR [31] | Topographic Map | Touching Text accuracy Low | 82% |
| Vectorization Algorithm [48] | Japan Meteorological Facsimile Maps | Not extracted full map Numbers | 92% |
| Pattern Recognition [32] | Chinese land register maps. | limited to very simple Map | 90% |
| Segmentation [33] | cadastral maps | Not good recognition of numeric character | |
| OCR with ANN [34] | Topographic Map | Poor recognition of text | 93% |
| **Proposed** | Any kind of | Recognition of | 90%-96% |

Spectrum of Engineering Sciences
Online ISSN 3007-3138
Print ISSN 3007-312X

| | | |
|---|---|---|
| **Method** | weather facsimile map | Unwanted Infrormations |

## 6. Conclusion

This research investigation explored the application of deep learning for the identification of line-shaped weather data derived from a meteorological facsimile map. To the best of our knowledge, a deep CNN has been utilized for the first time to tackle line-shaped meteorological weather maps. This effective application has the potential to address various pattern recognition challenges within meteorology. Deep neural networks acquire high-level representations from data directly, thereby potentially circumventing conventional and subjective thresholding methods for recognizing meteorological information. The findings from this study will serve to quantify specific information in the field of meteorology. Furthermore, this study provides an overview of the fundamental approaches within the CR domain, aiming to highlight the current state of research in this field. While each of the methods discussed has its unique strengths and weaknesses, they all attain a certain level of success. The character recognition algorithm demonstrated the highest reported accuracy in recognition. The combination methods proposed in this paper yield the most favourable outcomes among the recorded works.

## References

1. Wang, Y., et al., *Visual navigation systems for maritime smart ships: A survey*. Journal of Marine Science and Engineering, 2024. **12**(10): p. 1781.

Spectrum of Engineering Sciences
SPECTRUM OF ENGINEERING SCIENCES
Online ISSN
3007-3138
Print ISSN
3007-312X

2. Łącki, M., *Determining the Level of Threat in Maritime Navigation Based on the Detection of Small Floating Objects with Deep Neural Networks*. Sensors, 2024. **24**(23): p. 7505.
3. TEUCEANU, R., *THE PORTFOLIO OF OLD MAPS" SAMMLUNG AUSSEREUROPÄISCHER KARTEN (NO. 430)" IN THE BRUKENTHAL CARTOGRAPHIC CABINET*. Acta Musei Brukenthal, 2024. **19**(1).
4. Glahn, H.R., *50 years of model interpretation at the Meteorological Development Laboratory*. 2022.
5. Suter, M., *Early Macroseismic Intensity Observations, Isoseismal Maps, and Instrumental Recordings of Earthquakes in Mexico (1888–1934): A Review*. Seismological Research Letters, 2025.
6. Kim, J., et al. *N-imagenet: Towards robust, fine-grained object recognition with event cameras*. in *Proceedings of the IEEE/CVF international conference on computer vision*. 2021.
7. Verma, S., et al., *Deep learning techniques in extreme weather events: A review*. arXiv preprint arXiv:2308.10995, 2023.
8. Archana, R. and P.E. Jeevaraj, *Deep learning models for digital image processing: a review*. Artificial Intelligence Review, 2024. **57**(1): p. 11.
9. Niebler, S., et al., *Automated detection and classification of synoptic-scale fronts from atmospheric data grids*. Weather and Climate Dynamics, 2022. **3**(1): p. 113-137.
10. Arulananth, T., et al., *Edge detection using fast pixel based matching and contours mapping algorithms*. Plos one, 2023. **18**(8): p. e0289823.

Spectrum of Engineering Sciences
SPECTRUM OF ENGINEERING SCIENCES
Online ISSN
3007-3138
Print ISSN
3007-312X

11. Wang, Y., et al., *A method for tomato plant stem and leaf segmentation and phenotypic extraction based on skeleton extraction and supervoxel clustering*. Agronomy, 2024. **14**(1): p. 198.
12. Lv, Z., et al., *Blocknet: Beyond reliable spatial digital twins to parallel metaverse*. Patterns, 2022. **3**(5).
13. Xie, M., S. Xing, and J.M. Ahamada. *Research on detection and identification method of general air pressure system on marine weather chart*. in *Fourth International Conference on Computer Graphics, Image, and Virtualization (ICCGIV 2024)*. 2024. SPIE.
14. Bartoněk, D. and P. Andělová, *Method for cartographic symbols creation in connection with map series digitization*. ISPRS International Journal of Geo-Information, 2022. **11**(2): p. 105.
15. Li, Y. and Y. Tang, *Design on intelligent feature graphics based on convolution operation*. Mathematics, 2022. **10**(3): p. 384.
16. Trümper, L., et al. *Automatic mapping of parallel pattern-based algorithms on heterogeneous architectures*. in *International Conference on Architecture of Computing Systems*. 2021. Springer.
17. Alabdullah, B.I., et al., *Smart home automation-based hand gesture recognition using feature fusion and recurrent neural network*. Sensors, 2023. **23**(17): p. 7523.
18. Kukreja, V. and Sakshi, *Machine learning models for mathematical symbol recognition: A stem to stern literature analysis*. Multimedia Tools and Applications, 2022. **81**(20): p. 28651-28687.
19. Yin, Z., et al., *Mapping high-resolution basal topography of West Antarctica from radar data using non-stationary multiple-point*

Spectrum of Engineering Sciences
SPECTRUM OF ENGINEERING SCIENCES
Online ISSN
3007-3138
Print ISSN
3007-312X

*geostatistics (MPS-BedMappingV1).* Geoscientific Model Development Discussions, 2021. **2021**: p. 1-35.

20. Wang, Y., et al., *An automatic algorithm for estimating tropical cyclone centers in synthetic aperture radar imagery.* IEEE Transactions on Geoscience and Remote Sensing, 2021. **60**: p. 1-16.
21. Rivers, B.C., et al., *Bathymetric contour maps, surface area and capacity tables, and bathymetric change maps for selected water-supply lakes in northeastern Missouri, 2021*. 2023, US Geological Survey.
22. Ge, Y., et al. *Contributions of shape, texture, and color in visual recognition*. in *European Conference on Computer Vision*. 2022. Springer.
23. Sharma, R. and M. Ravinder, *Remote sensing image segmentation using feature based fusion on FCM clustering algorithm.* Complex & Intelligent Systems, 2023. **9**(6): p. 7423-7437.
24. AGBO, C., *SEGMENTATION OF HIGH-RESOLUTION SATELLITE IMAGERY USING A HYBRIDIZATION OF COLOUR-BASEDAND K-MEANS CLUSTERING TECHNIQUES FOR RESCUE MISSION*. 2023.
25. Magnier, B., et al. *A multi-scale line feature detection using second order semi-gaussian filters*. in *International Conference on Computer Analysis of Images and Patterns*. 2021. Springer.
26. Schult, J., et al., *Mask3d: Mask transformer for 3d semantic instance segmentation.* arXiv preprint arXiv:2210.03105, 2022.
27. Smit, F.W. and M.J. Welch, *Improved visualization of structural deformation on the Kraka structure (Danish Central Graben) with*

Spectrum of Engineering Sciences
Online ISSN
3007-3138
Print ISSN
3007-312X

*color-processed seismic data*, in *Geomechanical Controls on Fracture Development in Chalk and Marl in the Danish North Sea: Understanding and Predicting Fracture Systems*. 2023, Springer. p. 47-81.

28. Raatikainen, M., P. Sarala, and J.-P. Ranta, *Self-organizing map modelling and prospectivity mapping of surface geochemical data in Au and multi-metal mineral exploration: example from northern Finland*. Geochemistry: Exploration, Environment, Analysis, 2025. **25**(1): p. geochem2024-055.
29. Huang, W., et al., *Leveraging deep convolutional neural network for point symbol recognition in scanned topographic maps*. ISPRS International Journal of Geo-Information, 2023. **12**(3): p. 128.
30. Yang, J., et al., *An Automatic Derivation Method for Creation of Complex Map Symbols in a Topographic Map*. ISPRS International Journal of Geo-Information, 2023. **12**(3): p. 103.
31. Cao, R. and C.L. Tan. *Text/graphics separation in maps*. in *International Workshop on Graphics Recognition*. 2001. Springer.
32. Rao, X., et al., *Deep-learning-based annotation extraction method for chinese scanned maps*. ISPRS International Journal of Geo-Information, 2023. **12**(10): p. 422.
33. Vafaeinejad, A., et al., *Super-resolution AI-based approach for extracting agricultural cadastral maps: Form and content validation*. IEEE Journal of Selected Topics in Applied Earth Observations and Remote Sensing, 2025.

Spectrum of Engineering Sciences
Online ISSN
3007-3138
Print ISSN
3007-312X

34. Jain, P.H., et al., *Artificially intelligent readers: an adaptive framework for original handwritten numerical digits recognition with OCR Methods*. Information, 2023. **14**(6): p. 305.
35. Ghosh, M., et al., *Scene text understanding: recapitulating the past decade*. Artificial Intelligence Review, 2023. **56**(12): p. 15301-15373.
36. Samy, A., et al., *NanoVar: a comprehensive workflow for structural variant detection to uncover the genome's hidden patterns*. Nature protocols, 2025: p. 1-26.
37. Bhowmik, S., *Document region classification*, in *Document Layout Analysis*. 2023, Springer. p. 43-65.
38. Song, W., P. Li, and M. Wang, *Transmission line detection based on improved hough transform*. arXiv preprint arXiv:2402.02761, 2024.
39. Mulyana, T.M.S., et al., *Building Drawing Line Art with High Pass Filtering and Image Morphology*.
40. Saïd, F., et al., *The NOAA track-wise wind retrieval algorithm and product assessment for CyGNSS*. IEEE Transactions on Geoscience and Remote Sensing, 2021. **60**: p. 1-24.
41. Meister, P., et al., *Designing three-dimensional augmented reality weather visualizations to enhance general aviation weather education*. IEEE Transactions on Professional Communication, 2022. **65**(2): p. 321-336.
42. Robinson, E.L., et al., *CHESS-SCAPE: Future projections of meteorological variables at 1 km resolution for the United Kingdom 1980-2080 derived from UK Climate Projections 2018*. 2022.
43. Hirahara, S., et al., *Japan meteorological agency/meteorological research institute coupled prediction system version 3 (JMA/MRI–*

Spectrum of Engineering Sciences
Online ISSN
3007-3138
Print ISSN
3007-312X

*CPS3)*. Journal of the Meteorological Society of Japan. Ser. II, 2023. **101**(2): p. 149-169.

44. Job, M.S., et al., *Fractional rectified linear unit activation function and its variants*. Mathematical Problems in Engineering, 2022. **2022**(1): p. 1860779.
45. Azad, R., et al., *Medical image segmentation review: The success of u-net*. IEEE Transactions on Pattern Analysis and Machine Intelligence, 2024.
46. Waoo, A.A. and B.K. Soni, *Performance analysis of sigmoid and relu activation functions in deep neural network*, in *Intelligent Systems: Proceedings of SCIS 2021*. 2021, Springer. p. 39-52.
47. Pattanayak, B.K., et al. *A novel technique for handwritten text recognition using easy OCR*. in *2023 International Conference on Self Sustainable Artificial Intelligence Systems (ICSSAS)*. 2023. IEEE.
48. Kruger, R., et al., *Accessible computing*. ACM Trans, 2023. **16**(2).